9C.2

CHARACTERISTICS OF TROPICAL CYCLONE RAPID INTENSIFICATION IN ENVIRONMENTS OF UPPER-TROPOSPHERIC TROUGHS

Michael S. Fischer*, Brian H. Tang, and Kristen L. Corbosiero
University at Albany, SUNY

1. INTRODUCTION

Tropical cyclone (TC) intensification involves the interaction of processes on a wide spectrum of spatial and temporal scales, and has proven challenging to predict. TC intensity forecast errors can be especially large for rapid intensification (RI) events (Sampson et al. 2011; Emanuel and Zhang 2016). Compounding these issues, TCs that rapidly intensify prior to landfall are especially dangerous. Accordingly, the National Hurricane Center (NHC) has recently made the prediction of RI episodes its top forecast priority (Rappaport et al. 2012).

Environmental forcings, such as those from upper-tropospheric troughs, can play important roles in TC intensity change, including RI. Upper-tropospheric troughs may provide a source of eddy flux convergence of angular momentum (Molinari and Vollaro 1989; DeMaria et al. 1993; Peirano et al. 2016), as well as quasigeostrophic (QG) forcing for ascent (Bracken and Bosart 2000; Fischer et al. 2017), both of which can act to intensify the TC. Conversely, upper-tropospheric troughs can also be associated with unfavorable environmental conditions, such as increased vertical wind shear and dry air (DeMaria et al. 1993; Peirano et al. 2016).

Although a recent TC–trough climatology demonstrated that environments with a nearby upper-tropospheric trough tend to be less favorable for TC intensification (Peirano et al. 2016), some TC–trough interaction events still undergo RI. The goal of this work is to determine if certain TC–trough interaction configurations are more favorable for RI. Additionally, this analysis will explore whether RI episodes are associated with unique environmental characteristics compared to non-RI episodes of similar TC–trough configurations.

2. METHODOLOGY

Overwater TC intensity change episodes in the North Atlantic basin between 1989–2016 were compiled from the NHC "best track" hurricane database (Landsea and Franklin 2013). Environmental conditions were obtained from the ERA-Interim reanalysis (Dee et al. 2011). TCs were classified as being in one of three environmental groups, based on the maximum potential vorticity (PV) anomaly within a 250–1000-km storm-centered annulus, the distribution of which is shown in Fig. 1. The focus of this analysis is on those TCs in high-PV environments, characterized by maximum PV anomalies ≥ 2.0 PV units (PVU), and comprise the upper tercile of the distribution. These TCs were consistently found to be interacting with coherent upper-tropospheric troughs in a case-by-case analysis.

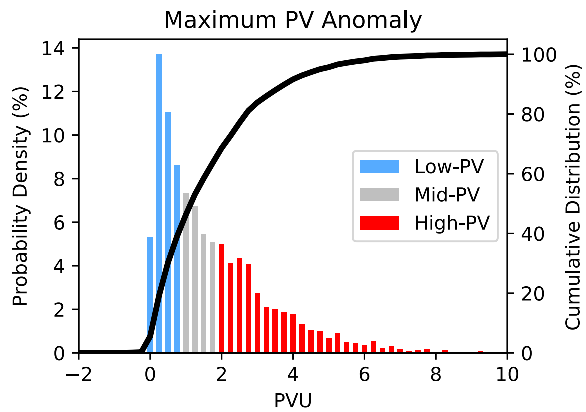

Figure 1. *Distribution of the maximum PV anomaly (PVU) on the 350-K isentropic surface within a 250–1000-km annulus for TCs in the North Atlantic. The probability density (%; binned every 0.25 PVU) is given by the bars, while the cumulative distribution (%) is represented by the black line. TCs in low-PV, mid-PV, and high-PV environments are represented by blue, gray, and red bars, respectively.*

To identify similar TC–trough configurations, PV anomalies on the 350-K isentropic surface were first interpolated onto a 1000×1000-km storm-centered grid with a spatial resolution of 50 km. Utilizing the PV anomalies at each grid point, a dimensionality reduction technique, t-Distributed Stochastic Neighbor Embedding (t-SNE; van der Maaten 2008), was implemented. t-SNE is a machine learning technique that can identify nonlinear relationships within a high-dimensional dataset; thus, it is well-suited for identifying similar upper-tropospheric configurations. The t-SNE algorithm allows each TC–trough interaction episode to be visualized as a point in a new two-dimensional space (Fig. 2a), with points located close together representing similar TC–trough configurations. Groups of similar TC–trough configurations were objectively identified using a k-means clustering algorithm on the t-SNE results. Since k-means clustering requires the number of

* *Corresponding author address*: Michael S. Fischer, Univ. at Albany, SUNY, Dept. of Atmospheric and Environmental Sciences, Albany, NY, 1400 Washington Ave., 12222; e-mail: msfischer@albany.edu

clusters to be specified beforehand, the number of clusters (three) that maximized the silhouette score, a measure of cluster cohesiveness, was selected for this analysis (Fig. 2b).

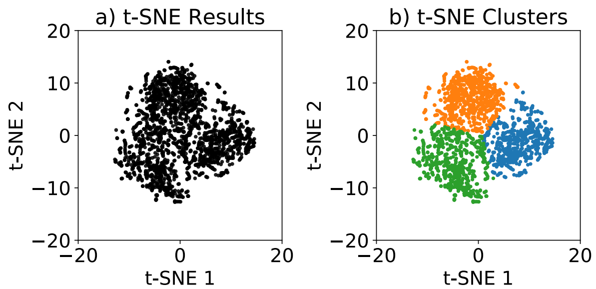

Figure 2. *(a) Scatter plots of the two-dimensional representation of 350-K PV anomalies using t-Distributed Stochastic Neighbor Embedding. (b) As in (a), but results are grouped by a k-means clustering algorithm. Blue, orange, and green dots, represent TC–trough interactions in Clusters 1, 2, and 3, respectively.*

3. RESULTS

Storm-centered composites of PV anomalies on the 350-K isentropic surface using the three clusters resulting from t-SNE are shown in Fig. 3. Each cluster is characterized by a unique TC–trough configuration. Cluster 1 TCs feature the largest upper-tropospheric PV anomaly, located nearest to, and to the south of, the TC (Fig. 3a). In Clusters 2 and 3, the upper-tropospheric trough is located to the northwest, and northeast, of the TC, respectively (Figs. 3b,c).

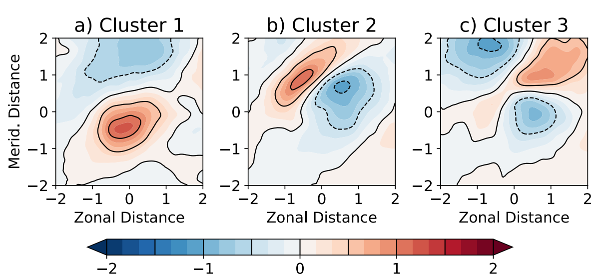

Figure 3. *Composite-mean, storm-centered, PV anomalies (PVU; shaded, with black contours drawn every 0.5 PVU) on the 350-K isentropic surface for high-PV TCs in the North Atlantic basin. TCs are grouped by the results shown in Fig. 2 using k-means clustering in conjunction with t-Distributed Stochastic Neighbor Embedding. The zonal and meridional distance (10^3 km) from the composite TC center are displayed along the axes.*

Within each cluster, TCs were placed into one of two intensity change groups, based on the 24-h change in maximum sustained 10-m wind (ΔV_{max}). TCs with a $\Delta V_{max} \geq 25$ kt were classified as RI episodes, consistent with the 95th percentile of ΔV_{max} for high-PV TCs. Otherwise TCs were classified as non-RI episodes. Cluster 1 TCs are associated with statistically significantly greater rates of intensity change than TCs in Clusters 2 and 3, and the highest fraction of storms that undergo RI (Fig. 4).

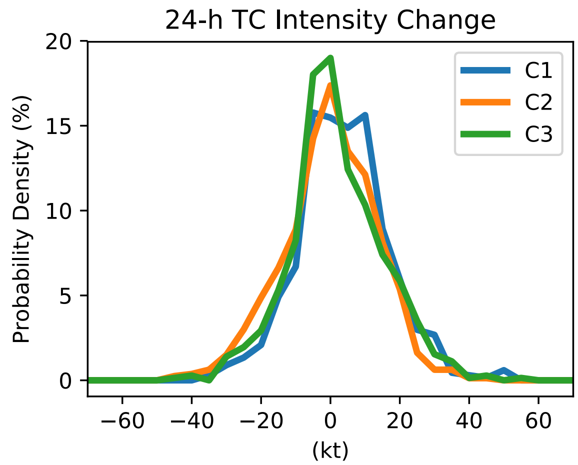

Figure 4. *Probability density (%) of 24-h TC intensity change (kt) for high-PV TCs in the North Atlantic basin from 1989–2016. The intensity change distributions are grouped by the TC–trough configuration cluster, where TCs in Clusters 1, 2, and 3 are represented by blue, orange, and green lines, respectively.*

The differences between RI and non-RI episodes among multiple environmental parameters were analyzed. For example, the distributions of the coupling index (CI), defined as

$$CI = \theta_{e,200} - \theta_{e,850} \qquad (1)$$

where $\theta_{e,200}$ and $\theta_{e,850}$ are the 200–800-km storm-centered, area-averaged, equivalent potential temperatures at 200 and 850 hPa, respectively, are shown in Fig. 5a. In each cluster, RI episodes are associated with statistically significantly lower CI values than non-RI episodes, indicative of less vertical stability. Interestingly, prominent differences between clusters exist. Cluster 1 TCs are associated with the greatest vertical stability, despite being associated with the greatest intensification rates. In fact, the CI distribution for Cluster 1 RI episodes is more similar to non-RI episodes in Clusters 2 and 3. These results suggest the anomalous vertical stability, relative to the type of TC–trough configuration, may be more important for RI than simply the observed vertical stability. Conversely, the magnitudes of 1000–250-hPa vertical wind shear for RI episodes were consistently weaker than those observed in non-RI episodes (Fig. 5b). It is hypothesized that vertical wind shear consistently plays a limiting role in the rate of TC intensification, regardless of the type of TC–trough configuration.

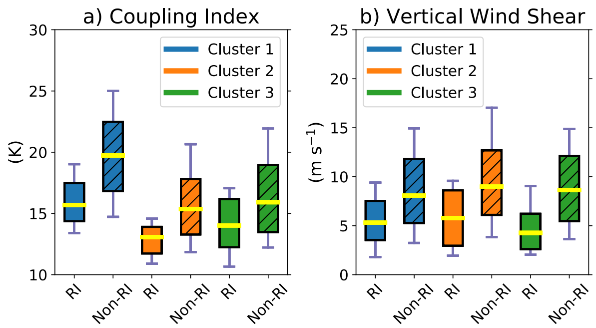

Figure 5. *Box and whisker plots of (a) CI (K) and (b) 1000–250-hPa vertical wind shear (m s^{-1}) for RI and non-RI episodes within Cluster 1 (blue), Cluster 2 (orange), and Cluster 3 (green), at the onset of the intensity change episode. The boxes range from the 25th–75th percentiles of the distribution, with a yellow line depicting the median, while the whiskers span the 10th–90th percentiles. Boxes with black hatching indicate the given intensity change group is associated with a statistically significantly different distribution from RI episodes within the corresponding cluster at the 95% confidence level.*

4. CONCLUSIONS

We have objectively identified three unique TC–trough configurations using a machine learning technique to analyze upper-tropospheric PV anomalies (Figs. 2 and 3). It was determined certain TC–trough configurations (Cluster 1) are associated with statistically significantly greater intensification rates, including RI (Fig. 4). RI TCs are consistently associated with more favorable environmental conditions than non-RI episodes of similar TC–trough configurations, however, the conditions considered to be favorable for RI can vary between clusters.

5. REFERENCES

Bracken, W. E., and L. F. Bosart, 2000: The role of synoptic-scale flow during tropical cyclogenesis over the North Atlantic Ocean. *Mon. Wea. Rev.*, **128**, 353–376.

Dee, D. P., and Coauthors, 2011: The ERA-Interim reanalysis: configuration and performance of the data assimilation system. *Quart. J. Roy. Meteor. Soc.*, **137**, 553–597.

DeMaria, M., J. Kaplan, and J.-J. Baik, 1993: Upper-level eddy angular momentum fluxes and tropical cyclone intensity change. *J. Atmos. Sci.*, **50**, 1133–1147.

Emanuel, K., and F. Zhang, 2016: On the predictability and error sources of tropical cyclone intensity forecasts. *J. Atmos. Sci.*, **73**, 3739–3747.

Fischer, M. S., B. H. Tang, and K. L. Corbosiero, 2017: Assessing the influence of upper-tropospheric troughs on tropical cyclone intensification rates after genesis. *Mon. Wea. Rev.*, **145**, 1295–1313.

Landsea, C.W., and J. L. Franklin, 2013: Atlantic hurricane database uncertainty and presentation of a new database format. *Mon. Wea. Rev.*, **141**, 3576–3592.

Molinari, J., and D. Vollaro, 1989: External influences on hurricane intensity. Part I: Outflow layer eddy angular momentum fluxes. *J. Atmos. Sci.*, **46**, 1093–1105.

Peirano, C.M., K. L. Corbosiero, and B. H. Tang, 2016: Revisiting trough interactions and tropical cyclone intensity change. *Geophys. Res. Lett.*, **43**.

Rappaport, E. N., J.-G. Jiing, C.W. Landsea, S. T.Murillo, and J. L. Franklin, 2012: The Joint Hurricane Test Bed: Its first decade of tropical cyclone research-to-operations activities reviewed. *Bull. Amer. Meteor. Soc.*, **93**, 371–380.

Sampson, C. R., J. Kaplan, J. A. Knaff, M. DeMaria, and C. A. Sisko, 2011: A deterministic rapid intensification aid. *Wea. Forecasting*, **26**, 579–585.

van der Maaten, L., and G. Hinton, 2008: Visualizing data using t-SNE. *J. Machine Learning Research*, **9**, 2579–2605.